

Enhanced low field magnetoresistance in nanocrystalline La_{0.7}Sr_{0.3}MnO₃ synthesized on MgO nanowires

Zhang, Zhen; Ranjith, R.; Xie, B. T.; You, L.; Wong, Lai Mun; Wang, Shijie; Wang, Junling;
Prellier, Wilfrid; Zhao, Y. G.; Wu, Tom

2010

Zhang, Z., Ranjith, R., Xie, B. T., You, L., Wong, L. M., Wang, S. J., et al. (2010). Enhanced low field magnetoresistance in nanocrystalline La_{0.7}Sr_{0.3}MnO₃ synthesized on MgO nanowires. *Applied Physics Letters*, 96.

<https://hdl.handle.net/10356/94263>

<https://doi.org/10.1063/1.3432113>

© 2010 American Institute of Physics. This paper was published in *Applied Physics Letters* and is made available as an electronic reprint (preprint) with permission of American Institute of Physics. The paper can be found at the following DOI:

<http://dx.doi.org/10.1063/1.3432113>. One print or electronic copy may be made for personal use only. Systematic or multiple reproduction, distribution to multiple locations via electronic or other means, duplication of any material in this paper for a fee or for commercial purposes, or modification of the content of the paper is prohibited and is subject to penalties under law.

Enhanced low field magnetoresistance in nanocrystalline $\text{La}_{0.7}\text{Sr}_{0.3}\text{MnO}_3$ synthesized on MgO nanowires

Z. Zhang,¹ R. Ranjith,² B. T. Xie,³ L. You,⁴ L. M. Wong,⁵ S. J. Wang,⁵ J. L. Wang,⁴ W. Prellier,² Y. G. Zhao,³ and T. Wu^{1,a)}

¹Division of Physics and Applied Physics, School of Physical and Mathematical Sciences, Nanyang Technological University, Singapore 637371

²Laboratoire CRISMAT, ENSICAEN, UMR 6508, CNRS, 6 Boulevard du Maréchal Juin, F-14050 Caen Cedex, France

³Department of Physics, Tsinghua University, Beijing 100084, People's Republic of China

⁴Division of Materials Science, School of Materials Science and Engineering, Nanyang Technological University, Singapore 639798

⁵Institute of Materials Research and Engineering, 3 Research Link, Singapore 117602

(Received 17 March 2010; accepted 27 April 2010; published online 1 June 2010)

We report on the structure and transport properties of nanocrystalline manganite $\text{La}_{0.7}\text{Sr}_{0.3}\text{MnO}_3$ (LSMO) synthesized on nanowires-engineered MgO substrates by pulsed laser deposition, which is compared with reference samples deposited directly on flat MgO substrates. Such LSMO/MgO nanocomposites show enhanced low field magnetoresistance, especially at low temperature, due to the dominant spin-polarized intergrain tunneling. This work suggests that growing on nanoengineered substrates is a viable route to achieve nanostructured materials with desired crystalline structure and physical properties. © 2010 American Institute of Physics. [doi:10.1063/1.3432113]

Manganites are prominent members in the strongly correlated electron systems and have attracted lots of interest in the recent decades.¹ $\text{La}_{0.7}\text{Sr}_{0.3}\text{MnO}_3$ (LSMO) is a stereotypical manganite with T_C above room temperature. In manganites, applied magnetic field shifts the metal-insulator transition to higher temperature, leading to the well known colossal magnetoresistance (CMR).² However, a high magnetic field (>1 T) is usually required to produce CMR, thus limiting the applications. Previous studies indicate that enhanced low field MR can be achieved at high frequencies or in polycrystalline manganites with small grains.³⁻⁵ In bulk ceramic synthesis, controlling the solid state reaction temperature and the quenching process are often used to tailor the grain size,^{2,5} whereas in thin films the purpose is usually fulfilled by strain engineering or using polycrystal substrates.^{4,6} Recently, Moshnyaga *et al.*⁷ reported that the structural phase transition could be manipulated in epitaxial manganite/MgO nanocomposite films and large CMR was acquired at the percolation threshold.

In exploration of the emerging physics in complex materials, combining bottom-up nanomaterials growth with conventional thin film techniques has emerged as an effective approach to achieve hierarchically structured nanomaterials and functional devices.^{8,9} In conventional thin film growth, sufficient diffusion barrier can induce the transition from the two-dimensional (2D) layer-by-layer mode to the three-dimensional island-growth mode.¹⁰ The characteristics of diffusion and nucleation during growth can be significantly modified if the flat substrate surface is engineered with predesigned nanostructures, thus rich growth behaviors and resulting morphologies are expected. Recently, this paradigm of materials synthesis has received increasing attention. For example, Nagashima *et al.*¹¹ deposited titanate on MgO

nanowires (NWs) and studied in detail the growth behaviors. From the theoretical perspective, Wang *et al.*¹² have analyzed the morphological stability of heterogeneous growth on NWs and found a growth regime analogous to the Stranski-Krastanow mode in conventional epilayers synthesis.

In this letter, we deposited LSMO on MgO NW arrays by using pulsed laser deposition (PLD) to achieve nanocrystalline films with uniform grain structure. Low field MR reaches -32% (5 kOe, 10 K) in these nanoengineered LSMO thin films, which is among the highest reported values. This approach combining NW synthesis and thin film techniques posits as a viable route to produce nanocrystalline oxides with predesigned structural and physical properties.

In typical experiments, MgO NW arrays were first grown on (100)-oriented MgO substrates via a vapor transport method at 900 °C in a tube furnace, and the details of the setup were given in previous reports.^{9,13} Catalyzed by Au nanoparticles, vertical MgO NWs were epitaxially grown on the substrates via the vapor-liquid-solid mechanism.¹⁴ This growth produces nanoengineered MgO substrates with 2D arrays of MgO NWs with uniform diameter (~ 40 nm), height (~ 300 nm), and density ($\sim 10^{10}$ cm⁻²). Then LSMO was deposited by PLD, as illustrated in Fig. 1(a). For comparison, LSMO thin film was also fabricated directly on flat MgO substrate as the “reference sample.” A nominal thickness of 300 nm was maintained in both cases. Au electrodes were sputter deposited for four-point transport measurements.

Insets in Fig. 1(a) show the scanning electron microscope (SEM) images of the well-aligned MgO NWs grown on MgO substrate. After PLD deposition, uniform nanocrystalline films with grain size <40 nm [Figs. 1(b) and 1(c)] were observed on the NWs. The NW density and the deposition rate were carefully chosen to produce uniform polycrystalline films. The growth morphology is in strong contrast to the reference sample deposited directly on flat MgO

^{a)}Electronic mail: tomwu@ntu.edu.sg.

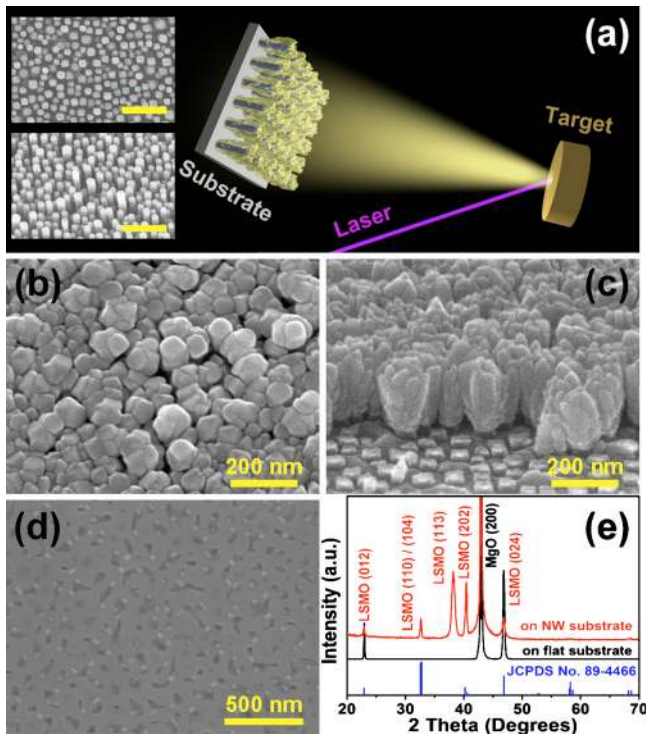


FIG. 1. (Color online) (a) Schematic illustrating the PLD deposition on NW-engineered substrate. Insets: top (upper) and 20° tilt (lower) SEM images of the MgO NW arrays. Scale bars: 200 nm. (b) and (c) Top and 20° tilt SEM images of the LSMO/NW sample. (d) SEM image of LSMO film deposited directly on flat MgO substrate (reference sample). (e) Corresponding XRD patterns.

substrates, where no well-defined grain was observed [Fig. 1(d)] and the structural defects in the form of nanopits are presumably the result of large lattice mismatch (9%). As shown in Fig. 1(e), the x-ray diffraction (XRD) pattern of the LSMO/NW sample confirms the polycrystalline rhombohedral LSMO structure ($a=5.50$ Å and $c=13.33$ Å, JCPDS: 89-4466). In comparison, the reference sample is (012) oriented, suggesting different growth behavior. Transmission electron microscope (TEM) images in Figs. 2(a) and 2(b) indicate that the LSMO/NW sample comprises of crystalline

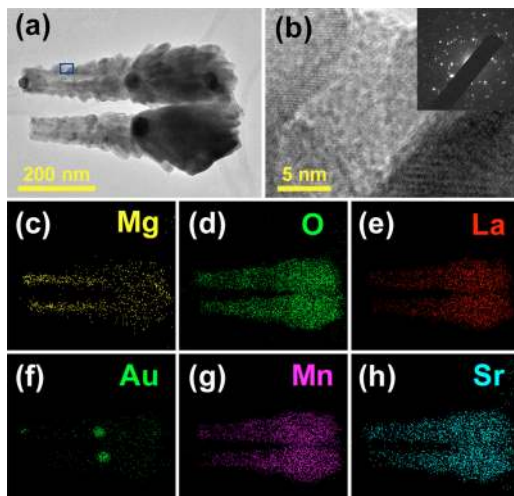


FIG. 2. (Color online) (a) TEM image of nanocrystalline LSMO coated on MgO NWs. (b) HRTEM image from the highlighted area in (a). Inset: SAED pattern. (c)–(h) Corresponding EDS element mappings. The weak Mg signal in (c) outside the MgO NW is an artifact.

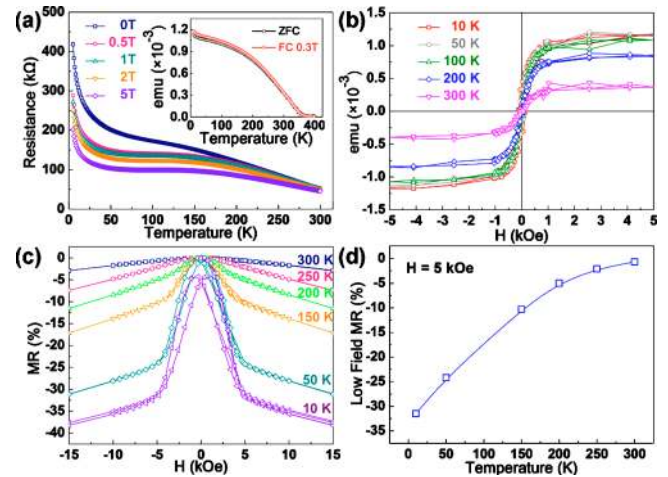


FIG. 3. (Color online) (a) $R-T$ data of the nanocrystalline LSMO/NW sample under various magnetic fields. Inset: $M-T$ data measured under both zero-field-cooled (ZFC) and field-cooled (FC) conditions with a magnetic field of 0.3 T. (b) Magnetic hysteresis loops measured at various temperatures. Inset shows the low field details. (c) $MR-H$ curves at various temperatures. (d) T-dependent MR at 5 kOe.

LSMO nanograins. The selected area electron diffraction (SAED, inset in Fig. 2(b)) also suggests a polycrystalline nature. Energy-dispersive x-ray spectroscopy (EDS) element mappings (Figs. 2(c)–2(h)) confirm the composition of the LSMO/NW heterostructure and show Au catalyst nanoparticles remaining on top of the MgO NWs.¹⁴

The resistance versus temperature ($R-T$) characteristics of the nanocrystalline LSMO/NW sample were measured under various magnetic fields (Fig. 3(a)), showing semiconductor or insulator-type behavior. Since the magnetism versus temperature ($M-T$) curves of the sample are bulk-like with $T_C \sim 355$ K (inset in Fig. 3(a)), we can conclude that the transport in the LSMO/NW sample is dominated by the spin-polarized tunneling at the grain boundaries, which is in line with the previous reports.^{2,4} The magnetic hysteresis loops are shown in Fig. 3(b), also suggesting ferromagnetic order in the whole temperature range. In the tunneling process, the spin polarization of electrons is preserved, and the misalignment of the magnetic moments between the neighboring grains gives rise to the large tunneling resistance.² The MR (defined as $[R(H)-R_{\max}]/R_{\max}$) versus magnetic field ($MR-H$) data were measured at various temperatures. As shown in Fig. 3(c), low field MR of -32% (5 kOe, 10 K) was achieved, which is among the highest reported values. In the high field regime (>5 kOe), the increment of MR slows down (Fig. 3(b)), but no saturation was observed even as the field reaches 5 Tesla.

The $R-T$ and $MR-H$ characteristics of the reference LSMO thin film deposited on the normal flat MgO substrate were measured for comparison. As depicted in Fig. 4(a), this sample shows the typical metallic $R-T$ behavior and its resistance is 4 to 5 orders lower than the nanocrystalline LSMO/NW sample. In addition, the MR of the reference sample is much smaller (-1.4% at 5 kOe and 300 K) and always proportional to the applied field (Fig. 4(b)).

The reduction of spin fluctuations by magnetic field should be responsible for the MR in the reference sample grown on flat MgO substrate.² In contrast, the enhanced low field MR of the nanocrystalline LSMO/NW film arises from the dominant spin-polarized tunneling across the grain

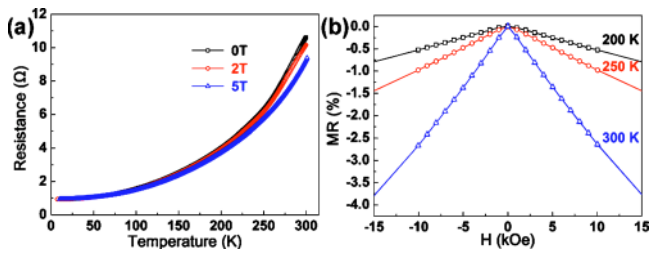


FIG. 4. (Color online) (a) R - T data of the LSMO thin film deposited on flat MgO substrate (reference sample). (b) MR - H curves at various temperatures.

boundaries.^{2,15} It has been shown that the intergrain dipolar coupling can reduce the tunneling MR of magnetic composites containing magnetic grains due to the paramagnetic feature of this interaction.¹⁶ However, the grains in the LSMO/NW sample are quite small, which weakens the intergrain dipolar interaction and favors the enhancement of the low field MR. Another important factor is the broken symmetry at the grain boundaries which may induce spin disorder at the grain boundaries¹⁷ and contribute to the high resistance at zero field. A magnetic field can align these disordered spins, thus reducing the tunneling barrier and giving the large MR.

In summary, nanocrystalline LSMO thin films were grown on NW-engineered MgO substrates by PLD. Enhanced low field MR, which reaches -32% at 5 kOe and 10 K, was acquired due to the dominant spin-polarized intergrain tunneling. Our result suggests that growing thin films on nano-engineered substrates is a viable route to achieve desired crystalline structure and physical properties.

We acknowledge support from the Singapore National Research Foundation (Grant No. NRF-G-CRP 2007-05), the C'Nano Nord Ouest (Grant No. GDR 2975), the Merlion (2.04.07) programs, the National 973 Project (Grant No. 2009CB929202), and the National Science Foundation of China (Grant No. 50872065).

¹W. Prellier, P. Lecoeur, and B. Mercey, *J. Phys.: Condens. Matter* **13**, R915 (2001); A. P. Ramirez, *ibid.* **9**, 8171 (1997); Y. Tokura, *Rep. Prog. Phys.* **69**, 797 (2006).

²H. Y. Hwang, S. W. Cheong, N. P. Ong, and B. Batlogg, *Phys. Rev. Lett.* **77**, 2041 (1996).

³A. Rebellio, V. B. Naik, and R. Mahendiran, *J. Appl. Phys.* **106**, 073905 (2009).

⁴N. D. Mathur, G. Burnell, S. P. Isaac, T. J. Jackson, B. S. Teo, J. L. MacManus-Driscoll, L. F. Cohen, J. E. Evetts, and M. G. Blamire, *Nature (London)* **387**, 266 (1997); C. Srinithiwarawong and M. Ziese, *Appl. Phys. Lett.* **73**, 1140 (1998); A. Gupta, G. Q. Gong, G. Xiao, P. R. Duncombe, P. Lecoeur, P. Trouilloud, Y. Y. Wang, V. P. Dravid, and J. Z. Sun, *Phys. Rev. B* **54**, R15629 (1996); I. Satoh and T. Kobayashi, *Jpn. J. Appl. Phys., Part 1* **40**, 586 (2001).

⁵C. L. Yuan, S. G. Wang, W. H. Song, T. Yu, J. M. Dai, S. L. Ye, and Y. P. Sun, *Appl. Phys. Lett.* **75**, 3853 (1999); S. I. Patil, A. S. Ogale, S. R. Shinde, D. C. Kundaliya, S. B. Ogale, S. M. Bhagat, and T. Venkatesan, *J. Appl. Phys.* **97**, 10H707 (2005).

⁶J. L. MacManus-Driscoll, P. Zerrer, H. Y. Wang, H. Yang, J. Yoon, A. Fouchet, R. Yu, M. G. Blamire, and Q. X. Jia, *Nat. Mater.* **7**, 314 (2008); Z. G. Sheng, Y. P. Sun, X. B. Zhu, W. H. Song, and P. Yan, *J. Phys. D: Appl. Phys.* **40**, 3300 (2007).

⁷V. Moshnyaga, B. Damaschke, O. Shapoval, A. Belenchuk, J. Faupel, O. I. Lebedev, J. Verbeeck, G. Van Tendeloo, M. Mucksch, V. Tsurkan, R. Tidecks, and K. Samwer, *Nat. Mater.* **2**, 247 (2003).

⁸D. Jian, P. X. Gao, W. J. Cai, B. S. Allimi, S. P. Alpay, Y. Ding, Z. L. Wang, and C. Brooks, *J. Mater. Chem.* **19**, 970 (2009); T. Wu and J. F. Mitchell, *Phys. Rev. B* **74**, 214423 (2006); A. Marcu, T. Yanagida, K. Nagashima, K. Oka, H. Tanaka, and T. Kawai, *Appl. Phys. Lett.* **92**, 173119 (2008).

⁹Z. Zhang, Y. H. Sun, Y. G. Zhao, G. P. Li, and T. Wu, *Appl. Phys. Lett.* **92**, 103113 (2008).

¹⁰J. Tersoff, A. W. Denier van der Gon, and R. M. Tromp, *Phys. Rev. Lett.* **72**, 266 (1994).

¹¹K. Nagashima, T. Yanagida, H. Tanaka, S. Seki, A. Saeki, S. Tagawa, and T. Kawai, *J. Am. Chem. Soc.* **130**, 5378 (2008).

¹²H. L. Wang, M. Upmanyu, and C. V. Ciobanu, *Nano Lett.* **8**, 4305 (2008).

¹³Z. Zhang, L. M. Wong, H. G. Ong, X. J. Wang, J. L. Wang, S. J. Wang, H. Y. Chen, and T. Wu, *Nano Lett.* **8**, 3205 (2008); Z. Zhang, J. Gao, L. M. Wong, J. G. Tao, L. Liao, Z. Zheng, G. Z. Xing, H. Y. Peng, T. Yu, Z. X. Shen, C. H. A. Huan, S. J. Wang, and T. Wu, *Nanotechnology* **20**, 135605 (2009); G. Z. Xing, J. B. Yi, D. D. Wang, L. Liao, T. Yu, Z. X. Shen, C. H. A. Huan, T. C. Sum, J. Ding, and T. Wu, *Phys. Rev. B* **79**, 174406 (2009); Z. Zhang, J. B. Yi, J. Ding, L. M. Wong, H. L. Seng, S. J. Wang, J. G. Tao, G. P. Li, G. Z. Xing, T. C. Sum, C. H. A. Huan, and T. Wu, *J. Phys. Chem. C* **112**, 9579 (2008).

¹⁴R. S. Wagner and W. C. Ellis, *Appl. Phys. Lett.* **4**, 89 (1964).

¹⁵S. Lee, H. Y. Hwang, B. I. Shraiman, W. D. Ratcliff, and S. W. Cheong, *Phys. Rev. Lett.* **82**, 4508 (1999).

¹⁶D. Kechrakos and K. N. Trohidou, *Phys. Rev. B* **71**, 054416 (2005); J. V. Lopes, J. dos Santos, and Y. G. Pogorelov, *ibid.* **66**, 064416 (2002).

¹⁷M. H. Zhu, Y. G. Zhao, W. Cai, X. S. Wu, S. N. Gao, K. Wang, L. B. Luo, H. S. Huang, and L. Lu, *Phys. Rev. B* **75**, 134424 (2007).